J Mater Sci: Mater Med (2009) 20:1653–1658
DOI 10.1007/s10856-009-3723-3

Silicon-substituted hydroxyapatite composite coating by using vacuum-plasma spraying and its interaction with human serum albumin

Feng-juan Xiao · Lei Peng · Ying Zhang · Li-jiang Yun

Received: 10 October 2008 / Accepted: 23 February 2009 / Published online: 20 March 2009

Abstract The incorporation of silicon can improve the bioactivity of hydroxyapatite (HA). Silicon-substituted HA ($Ca_{10}(PO_4)_{6-x}(SiO_4)_x(OH)_{2-x}$, Si-HA) composite coatings on a bioactive titanium substrate were prepared by using a vacuum-plasma spraying method. The surface structure was characterized by using XRD, SEM, XRF, EDS and FTIR. The bond strength of the coating was investigated and XRD patterns showed that Ti/Si-HA coatings were similar to patterns seen for HA. The only different XRD pattern was a slight trend toward a smaller angle direction with an increase in the molar ratio of silicon. FTIR spectra showed that the most notable effect of silicon substitution was that –OH group decreased as the silicon content increased. XRD and EDS elemental analysis indicated that the content of silicon in the coating was consistent with the silicon-substituted hydroxyapatite used in spraying. A bioactive TiO_2 coating was formed on an etched surface of Ti, and the etching might improve the bond strength of the coatings. The interaction of the Ti/Si-HA coating with human serum albumin (HSA) was much greater than that of the Ti/HA coating. This might suggest that the incorporation of silicon in HA can lead to significant improvements in the bioactive performance of HA.

F.-j. Xiao (✉) · L. Peng · Y. Zhang · L.-j. Yun
Department of Material Science and Engineering, Shjiazhuang Railway Institute, No.17 North 2nd-Ring East Road, Shijiazhuang 050043, Hebei Province, China
e-mail: xfj66@126.com

1 Introduction

Hydroxyapatite [$Ca_{10}(PO_4)_6(OH)_2$, HA] is the most popular bioactive material for medical applications due to its resemblance to the inorganic phase of natural bones. However, when compared with other bioactive materials, HA has a lower reaction rate with bone tissue. [1]. A titanium surface that is coated with HA can overcome the brittleness and poor mechanical performance of HA, and makes use of both the excellent biocompatibility of HA and the high mechanical strength of metallic materials [2]. Silicon is a trace element known to be essential in biological processes. The incorporation of silicon into HA is well known to improve its bioactivity [3].

Because the stability of an implanted region depends on the formation of a strong mechanical bond between the implant and the surrounding regions within the bone, it is desirable for the bone fiber to grow as quickly as possible. Si-HA can better increase the amount of bone tissue than can pure HA [4]. As a calcific agent, silicon enhances the growth rate of bone, improving the strength of the bond to bioactive prosthetic material. The importance of silicon in bone formation and calcification has been demonstrated through in vitro and in vivo studies [5–7]. Several studies report the preparation of pure HA coatings by using the electrophoretic deposition technique (EPD) and by using atmospheric plasma spraying. However, there are some disadvantages to those methods, such as weak bond strength between the coating and the substrate and the decomposition of HA into α-TCP and β-TCP [8, 9]. In a recent study, silicon-substituted hydroxyapatite was synthesized by using a hydrothermal method and the Ti/Si-HA coatings were prepared by vacuum-plasma spraying, where Si-HA powder was sprayed onto the titanium substrate. In this study, the morphology, composition and the

interactions with human serum albumin (HSA) of Si-HA were studied.

2 Experimental

Si-HA was prepared by using a hydrothermal synthesis method, employing the precipitation reaction between $Ca(NO_3)_2 \cdot 4H_2O$, $(NH_4)_2HPO_4$ (molar ratio $n_{Ca}/n_{(Si+P)} = 1.67$) and [Si $(CH_3CH_2O)_4$] for 12 h at 95°C with triethanolamine (TEA) as a surfactant. Titanium samples were abraded on 600-grit silicon carbide paper before spraying and were etched with a solution of 4% hydrofluoric acid and 3% nitric acid to form a TiO_2-bonding layer [10]. Si-HA coatings and pure HA coatings (HA was purchased from Sulzer Metco) were sprayed on the titanium substrate by using a vacuum-plasma spraying system (Sulzer Metco A2000). The spray parameters are listed in Table 1.

The elemental contents of HA and Si-HA were determined by using XRF (Philips PW-1606) and EDS (VGR-3), the crystal structure was characterized by using XRD (D8-Advance) and FTIR (330-FTIR) was used to analyze the functional groups in the crystals before and after the interaction of Ti/Si-HA coatings with HSA. The morphology and the thickness of the coatings were observed by using SEM (Kyky-2800). The bond strength of the coatings was tested by using an electronic multi-purpose tester (CSS-2210) according to the ASTM C-633 standard.

Table 1 Spray parameters

Plasma gas Ar	40 slpm powder	2.0 slpm Ar
Plasma gas H_2	10 slpm powder	Feed rate 20 g/min
Spray distance	300 mm	Current 650 A
Coating thickness	60 μm	Voltage 50 V
Chamber pressure	150 mbar	

3 Results and discussion

3.1 SEM observation

The morphology shown on the scanning electron micrograph of the Si-HA, as given in Fig. 1, suggested that the crystals were very well-distributed in size and that most of them were rod-like in shape. SEM also indicated that the particle widths were slightly reduced, and their lengths increased with an increasing amount of silicon, and the crystals' shapes were changed from rod-like into needle-like formations, similar to the HA crystals occurring in natural bones.

The morphology of the titanium and the Si-HA coatings are shown in Figs. 2 and 3. Figure 2 shows the surface of titanium treated by hydrofluoric acid and nitric acid. The titanium became much rougher and had an abundance of micropores, which helped to increase the surface area of the substrate and helped to form a mechanical interlock between the titanium and the Si-HA coating. Figure 3 shows the surface (a) and the cross-section (b) morphology of the coatings. The thickness of the coating was about 50 μm.

3.2 The content of Si on the coatings

The Si content of the coatings was investigated by using XRF and EDS. The coatings contained six elements: Ca, Si, P, Ti, O and Na. The presence of titanium and sodium may be attributed to the TiO_2 and Na_2TiO_3 in the coatings.

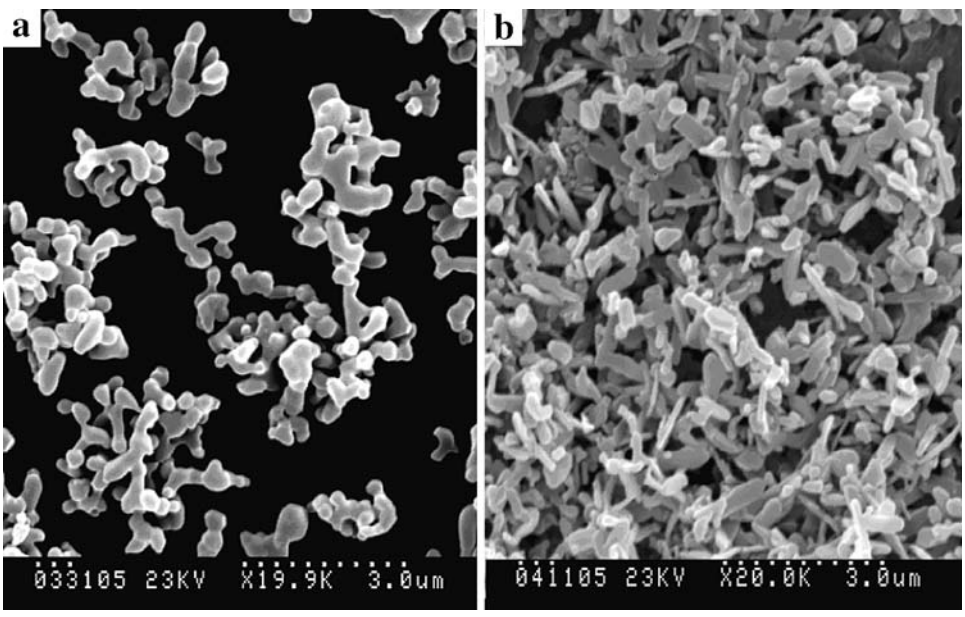

Fig. 1 SEM morphology of **a** 0.83 wt% and **b** 1.26 wt% Si-HA

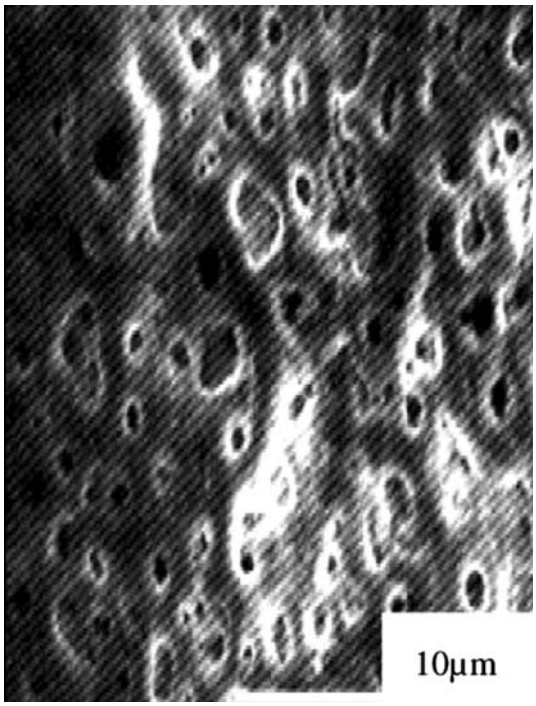

Fig. 2 SEM images of the surface morphology of Ti after bioactive treatment

The EDS spectra of the Ti/Si-HA coatings shown in Fig. 4 indicated that silicon peaks of Si-HA intensified with an increase in the silicon content. The molar ratio of silicon was 0.43, 0.81 and 1.22 wt% for the coating prepared from Si-HA powder containing 0.45, 0.86 and 1.26 wt% of Si, respectively. These results, coupled with previous studies [8], pave the way for the fabrication of deposits of graded composition and of laminates.

3.3 XRD analysis

The XRD patterns of Ti and of the coatings are shown in Fig. 5. After bioactive treatment, the titanium substrate showed characteristic diffraction peaks for TiO_2 at $2\theta = 25.30$, 36.85, 36.85 and 53.90 (JCPDS 78-2486), which suggested that a TiO_2 substrate structure was formed [11]. It was reported [12] that TiO_2 might enhance the bonding strength of the HA coating. The XRD patterns of the Ti/Si-HA coatings were similar to those of HA. The difference in their XRD patterns was a slight shift toward the small angle direction with an increase in the molar ratio of silicon. This indicated that the incorporation of silicon changed the lattice of the crystal, as was reported by

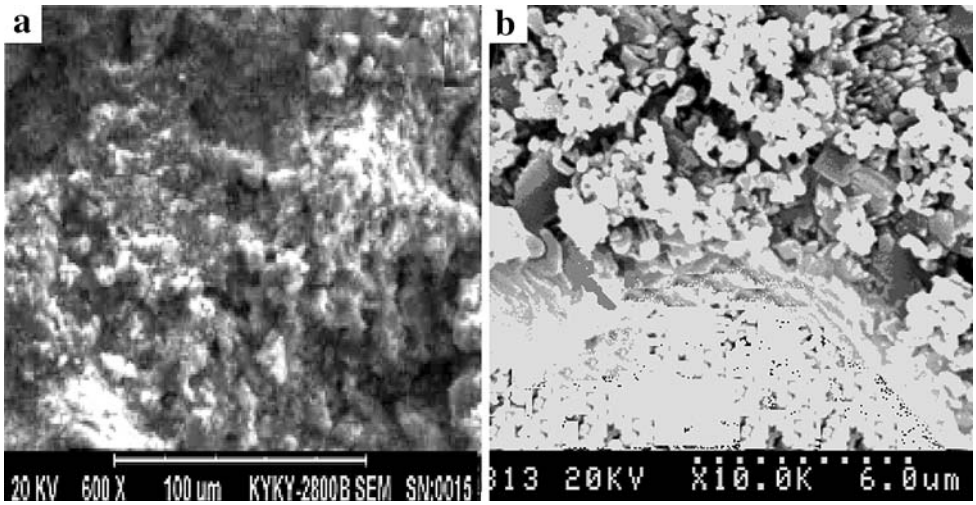

Fig. 3 SEM images of the surface (**a**) and cross-section (**b**) morphology of Ti/Si-HA coatings

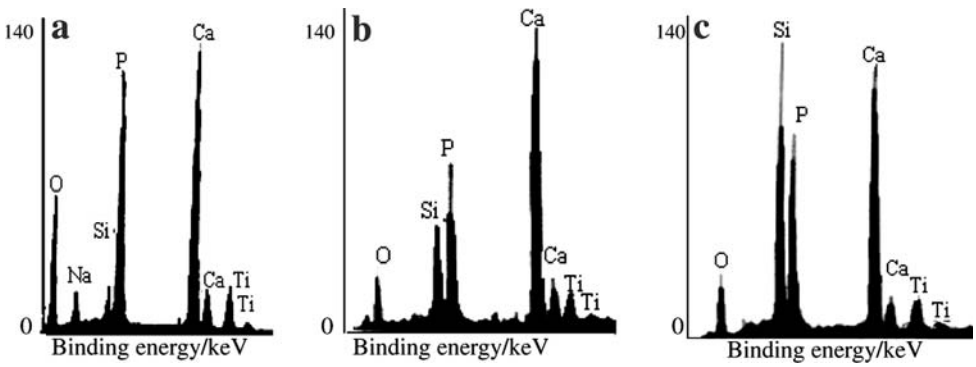

Fig. 4 EDS spectra of Ti/Si-HA coatings with different molar ratio of Si in Si-HA: **a** 0.45 wt%, **b** 0.81 wt% and (**c**) 1.22 wt%

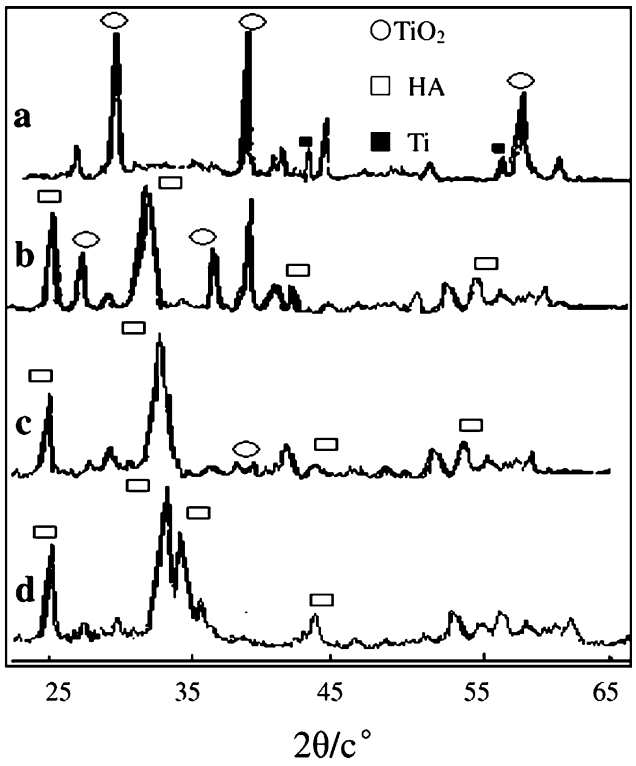

Fig. 5 XRD spectra of the surface of Ti and Ti/HA coating (a) Ti after bioactive treatment, (b) Ti/Si-HA coating (1.22 wt%), (c) Ti/Si-HA coating (0.81 wt%) and (d) pure Ti/HA coating

Gibson et al. [13]. As the radius of P^{5+} is smaller than that of Si^{4+}, and the bond length of P–O (O.155 nm) is shorter than that of Si–O (0.161 nm), the radius of the tetrahedrons PO_4^{3-} is smaller than that of SiO_4^4. The partial substitution of SiO_4^4 for PO_4^{3-} induced a shortening of the a-axis of the cell and induced an expansion of the c-axis [14], all of which resulted in a slight change in the cell structure.

3.4 FTIR analysis

The FTIR spectra of HA and Si-HA coatings are presented in Fig. 6. The weak hydroxyl group (–OH) band was at 3571 cm^{-1} and the H_2O bands were at 3500 and 1648 cm^{-1}. The phosphate stretching vibration bands were identified by peaks at 960 and 870 cm^{-1} and the bending vibration bands of phosphate were at 603 and 567 cm^{-1}. Compared with the pure HA coatings, the notable effects of silicon substitution on FTIR spectra were the changes in the –OH bands. Observation of the spectra, as a function of the silicon substitution, showed that the bands corresponding to –OH groups decreased with increased silicon substitution.

3.5 Bond strength of coating

The bond strength of the Ti/Si-HA coatings (molar ratio of Si = 1.22 wt%, with a thickness of 56 μm) with bioactive

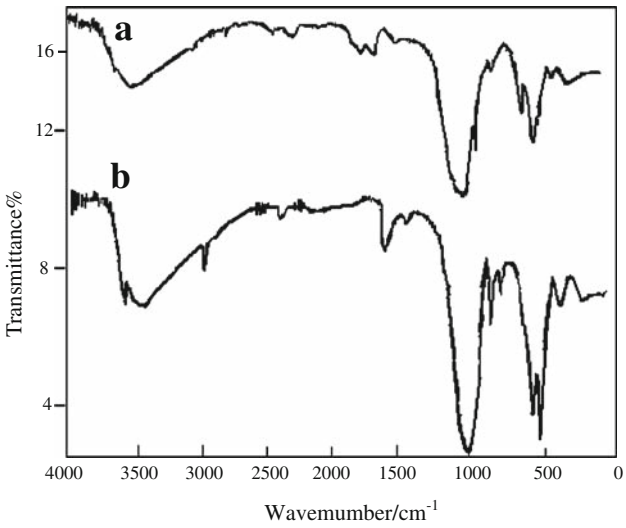

Fig. 6 FTIR patterns of the (a) Ti/Si-HA (1.22 wt%), (b) Ti/HA coating

treatment substrate was 25.6 Mpa, according to the ASTM C-633 standard.

By comparison, the bond strength of the coating without treatment was 16.7 Mpa. The tensile strength of the coating, with TiO_2 as the sublayer, was 21.3 Mpa. The formation of TiO_2 and the titanate layer might decrease the stress concentration and thermal expansion coefficient mismatch between the coatings and the titanium substrate [15], which has the advantage of improving the bond strength of the coatings.

3.6 Interaction of Ti/Si-HA coating with HSA

3.6.1 SEM morphologies of Ti/Si-HA coating after interaction with HSA

The coatings appeared to have a different morphology (Fig. 7) after interaction with HSA for 3 days. The surface of the coating had hairy and wadding shapes, and there were many tiny needle-shape structures growing on the surface of the coating. This suggested that the protein improved the ordering of the crystals, and that Si-HA might have dissolved in the HSA solution. The $CaPO_4^{3-}$ and SiO_4^{4-} in the Si-HA coating might dissolve, adsorb and then bond with HSA and reach equilibrium under certain conditions [16]. As the complicated interaction between the protein and HA induced the biomineralization process of Si-HA and formed a highly self-assembled structure, it might make the biomineralization samples possess the same chemical components as do bone tissues.

3.6.2 FTIR analysis of Ti/Si-HA coating after interaction with HSA

The FTIR spectra of Ti/Si-HA scraped powder showed (Fig. 8) amide group ($–CONH_2$) bands between 1700 and

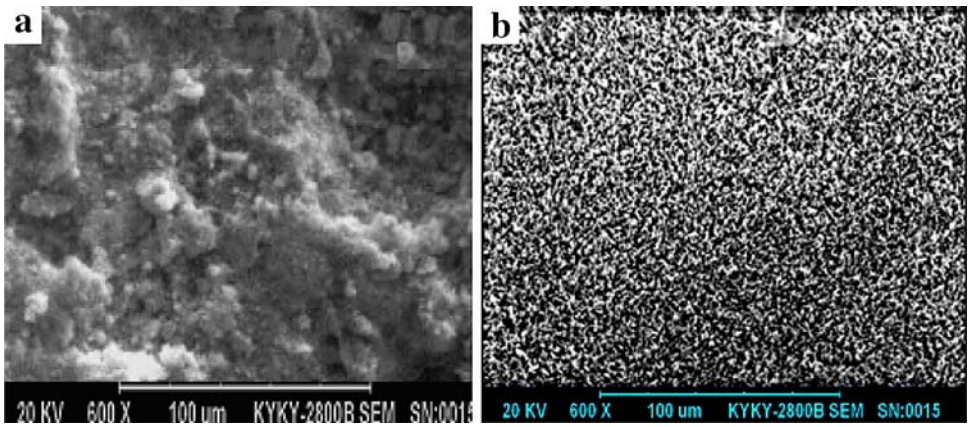

Fig. 7 SEM morphologies of Ti/Si-HA coating before (**a**) and after (**b**) reaction with HSA for 3 days

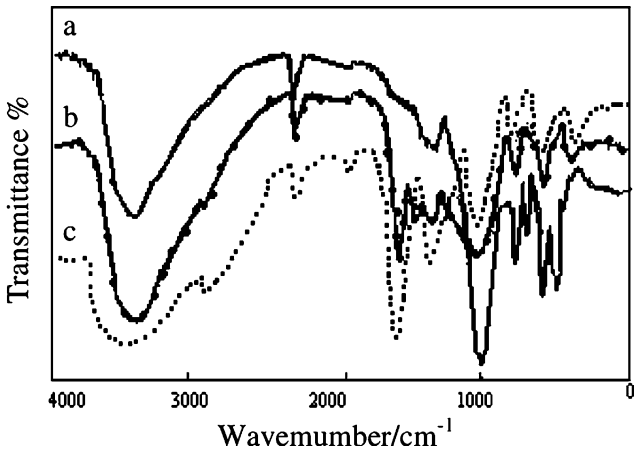

Fig. 8 FTIR patterns of Ti/Si-HA after interaction with HSA: **a** Ti/HA coating, **b** Ti/Si-HA containing 0.81 wt% Si; and **c** Ti/Si-HA containing 1.22 wt% Si

1600 cm^{-1} and in HAS an amide group band was observed at 1545 cm^{-1} [15]. Compared with the FTIR spectra of pure Ti/HA, the peak of the amide group of Ti/Si-HA was more intense. This suggested that the interaction of the Ti/Si-HA coating with HSA was much greater than that of Ti/HA, and that the incorporation of a small amount of silicon in the HA might improve the reactive performance of Ti/HA with HSA.

4 Conclusion

Ti/Si-HA coatings were prepared by vacuum-plasma spraying. The XRD spectra of the coating had patterns similar to HA, with a slight shift toward small angle direction. The most notable effect of silicon substitution on FTIR spectra was that the –OH groups decrease with an increase in silicon substitution. Silicon dopes in the crystal lattice of HA and the content of Si in the Ti/Si-HA coating was consistent with the Si-HA powder used in the spraying. The interaction of the Ti/Si-HA coating with HSA was much greater than that of the Ti/HA coating. This might suggest that the incorporation of a small amount of silicon into HA significantly improves the reactive performance of HA with protein.

References

1. Suchanek W, Yoshimura M. Processing and properties of hydroxyapatite-based biomaterials for use as hard tissue replacement implants. J Mater Res. 1998;13:94–117.
2. Sfidhar TM, Mudala UK, Subbaiyan M. Preparation and characterization of electrophoretically deposited hydroxyapatite coating on type 316L stainless steel. Corr Sci. 2003;45:237–52. doi:10.1016/S0010-938X(02)00091-4.
3. Zhitomirsky I, Galor L. Electrophoretic deposition of hydroxyapatite. J Mater Med. 1997;8:213–9.
4. Balas F, Perez PJ, Vallet RM. *In vitro* bioactivity of silicon-substituted hydroxyapatites. Biomaterials. 2003;24:3203–9.
5. Tang XL, Xiao XF, Liu RF. Structural characterization of silicon-substituted hydroxyapatite synthesized by a hydrothermal method. Mater Lett. 2005;59:3841–6. doi:10.1016/j.matlet.2005.06.060.
6. Thian ES, Huang J, Best SM, Barber ZH. Silicon-substituted hydroxyapatite: the next generation of bioactive coatings. Mater Sci Eng C. 2007;27:251–6. doi:10.1016/j.msec.2006.05.016.
7. Suzuki K, Yumura T, Mizuguchi M, et al. Apatite-silica gel composite materials prepared by a new alternate soaking process. J Sol–Gel Sci Technol. 2001;21:55–63.
8. Mondragon CZ, Vargas GG. Electrophoretic deposition of hydroxyapatite submicron particles at high voltages. Mater Lett. 2004;58:1336–9. doi:10.1016/j.matlet.2003.09.024.
9. Junichi HA, Yuki A, Kiyoshi K. Fabrication of highly ordered macroporous apatite coating onto titanium by electrophoretic deposition method. Solid State Ion. 2004;172:331–4. doi:10.1016/j.ssi.2004.02.046.
10. Wei M, Ruys AJ, Swain MV. Interfacial bond strength of electrophoretically deposited hydroxyapatite coatings on metals. J Mater Sci: Mater Med. 1999;10:401–9. doi:10.1023/A:1008923029945.
11. Niwa M, Wei L, Sato I. The adsorptive property of hydroxyapatite to albumin dextrin and lipids. Biomed Mater Eng. 1999;9:163–9.
12. Tanizawa Y, Suzuki T. X-ray photoelectron spectroscopy study of silicate-containing apatite. Phosphorus Res Bull. 1994;4:83–8.
13. Gibson IR, Best SM, Bonfield W. Chemical characterization of silicon-substituted hydroxyapatite. J Biomed Mater Res.

1999;4:422–8. doi:10.1002/(SICI)1097-4636(19990315)44:4<422::AID-JBM8>3.0.CO;2-#.
14. Le Ventouri TH, Bunaciu CE, Perdikatsis V. Neutron powder difraction studies of silicon-substituted hydroxyapatite. Biomaterials. 2003;24:4205–421. doi:10.1016/S0142-9612(03)00333-8.
15. Tao W-s, Li W, Jiang Y-M. The basic of protein molecules. 2nd ed. Beijing: Higher Education Press; 1995.
16. Yin G, Zhan J, Liu Z. Characterization of the adsorption of human serum albumin on hydroxylapatite. Chem J Chin Univ. 2002;22:771–5. J.